

Macroscale Thalamic Functional Organization Disturbances and Underlying Core Cytoarchitecture in Early-Onset Schizophrenia

Yun-Shuang Fan^{1,2}, Yong Xu⁸, Şeyma Bayrak², James M. Shine^{3,9}, Bin Wan^{2,5,7,9}, Haoru Li¹, Liang Li^{1,6}, Siqi Yang¹, Yao Meng¹, Sofie L. Valk^{2,5,9}, and Huafu Chen^{*,1,4,9}

¹The Clinical Hospital of Chengdu Brain Science Institute, School of Life Science and Technology, University of Electronic Science and Technology of China, Chengdu, China; ²Otto Hahn Group Cognitive Neurogenetics, Max Planck Institute for Human Cognitive and Brain Sciences, Leipzig, Germany; ³Brain and Mind Center, The University of Sydney, Sydney, Australia; ⁴MOE Key Lab for Neuroinformation, High-Field Magnetic Resonance Brain Imaging Key Laboratory of Sichuan Province, University of Electronic Science and Technology of China, Chengdu, China; ⁵Institute of Neuroscience and Medicine (INM-7: Brain and Behavior), Research Centre Jülich, Jülich, Germany; ⁶Academy for Advanced Interdisciplinary Studies, Peking University, Beijing, China; ⁷International Max Planck Research School on Neuroscience of Communication: Function, Structure, and Plasticity (IMPRS NeuroCom), Leipzig, Germany; ⁸Department of Psychiatry, First Hospital/First Clinical Medical College of Shanxi Medical University, Taiyuan, China

⁹Both last co-authors contributed equally.

*To whom correspondence should be addressed; fax: 086-028-83200131, e-mail: chenhf@uestc.edu.cn

Background and Hypothesis: Schizophrenia is a poly-genetic mental disorder with heterogeneous positive and negative symptom constellations, and is associated with abnormal cortical connectivity. The thalamus has a coordinative role in cortical function and is key to the development of the cerebral cortex. Conversely, altered functional organization of the thalamus might relate to overarching cortical disruptions in schizophrenia, anchored in development. **Study Design:** Here, we contrasted resting-state fMRI in 86 antipsychotic-naïve first-episode early-onset schizophrenia (EOS) patients and 91 typically developing controls to study whether macroscale thalamic organization is altered in EOS. Employing dimensional reduction techniques on thalamocortical functional connectome (FC), we derived lateral–medial and anterior–posterior thalamic functional axes. **Study Results:** We observed increased segregation of macroscale thalamic functional organization in EOS patients, which was related to altered thalamocortical interactions both in unimodal and transmodal networks. Using an ex vivo approximation of core-matrix cell distribution, we found that core cells particularly underlie the macroscale abnormalities in EOS patients. Moreover, the disruptions were associated with schizophrenia-related gene expression maps. Behavioral and disorder decoding analyses indicated that the macroscale hierarchy disturbances might perturb both perceptual and abstract cognitive functions and contribute to negative syndromes in patients. **Conclusions:** These findings provide mechanistic evidence for disrupted thalamocortical system in schizophrenia, suggesting a unitary pathophysiological framework.

Key words: cytoarchitectural/early-onset schizophrenia/functional hierarchy/genetic/thalamus

Introduction

Schizophrenia is a polygenetic psychiatric illness characterized by a combination of psychotic symptoms and motivational/cognitive deficits, which usually emerge during early adulthood.¹ Over the past 2 decades, a wealth of neuroimaging studies have indicated that schizophrenia can be associated with pathological interactions across widely distributed brain regions, instead of focal brain damages. Accordingly, the overarching dysconnection hypothesis posits that schizophrenia results from brain structural and functional connectivity abnormalities.² The thalamus, which is well-placed to arbitrate the interactions between distributed brain organization,³ might play a pivotal role in the pathophysiological process of schizophrenia.^{4,5}

The thalamus is a cytoarchitecturally heterogeneous diencephalic structure that contains an admixture of Parvalbumin (PVALB)-rich “Core” cells and Calbindin (CALB1)-rich “Matrix” cells.⁶ Whereas core cells preferentially target granular layers (Layers III and IV) of unimodal primary regions, such as primary visual, auditory, and somatosensory cortices, matrix cells target supragranular layers (Layers I–III) over wide areas in a diffuse pattern.⁷ This means that distinct thalamic cells may interact with cortical areas organized into different topological zones.⁸ Cellular-scale information of the

thalamus may be a critical factor to understand the thalamocortical interactions that supports cognition and behavior. Indeed, the thalamocortical system has been suggested to form the basis for binding multiple sensory experiences into a single framework of consciousness.⁹ By coordinating the modular architecture of cortical networks, the thalamus has been reported to be engaged in integrating information processing within the whole cerebral cortex.¹⁰

In accordance with its function coordinating cortical network organization, the thalamus plays the central role in the development of the cerebral cortex.¹¹ During brain development, the thalamus changes in concordance with the cerebral cortex and disturbances of this coordinated process relate to cognitive dysfunctions,¹² serving as a precursor of schizophrenia. Thalamocortical dysconnectivity patterns, mainly characterized by hyperconnectivity with sensorimotor areas and hypoconnectivity with prefrontal regions, have been reported in both pediatric¹³ and early-stage¹⁴ patients with schizophrenia. Clinically, thalamic hyperconnectivity with sensory regions was related to hallucinations and delusions,¹⁵ and hypoconnectivity with prefrontal regions was relevant to multiple symptom domains.¹⁶ The dysconnectivity pattern has been hypothesized to arise from disturbed brain maturation, particularly during the transition from youth to adulthood.¹⁷ Intriguingly, thalamo-prefrontal hypoconnectivity is correlated with thalamo-sensorimotor hyperconnectivity in psychotic patients, potentially implying a shared pathophysiological mechanism.¹⁸ However, few studies have investigated thalamocortical connectivity in the still developing brain of schizophrenia from a comprehensive perspective.

Recently, the application of dimension reduction techniques has emerged as a promising strategy for holistic representations of brain connectivity. These novel data-driven methods decompose high dimensional connectome into a series of low dimensional axes capturing spatial gradients of connectivity variations.^{19,20} The gradient framework describes a continuous coordinate system, in contrast to clustering-based methods resulting in discrete communities.²¹ Using these methods in the context of cortex-wide functional connectome (FC), previous studies observed a cortical hierarchy that spans from unimodal primary regions to transmodal regions,²² which has a close link with cortical microstructure like cytoarchitecture or myeloarchitecture.²³ Their coupling along the unimodal–transmodal axis has been reported to be genetically- and phylogenetically-controlled, supporting flexible cognitive functions.²⁴ Perturbed macroscale cortical functional hierarchies have been reported in various neurological^{25,26} and psychiatric disorders²¹ including schizophrenia.²⁷ Also, thalamic hierarchies have been previously derived from thalamocortical connectome, identifying a lateral–medial (L–M) principal gradient and an anterior–posterior (A–P) secondary gradient.²⁸ The L–M axis

captures thalamic anatomical nuclei differentiation, while the A–P axis characterizes unimodal–transmodal functional hierarchy. Also the coupling between core-matrix cytoarchitecture and FC has been shown to describe the unimodal–transmodal cortical gradients, and argued to play a major role in shaping functional dynamics within the cerebral cortex.⁸ Given the possible implication of the thalamus in schizophrenia, thalamic hierarchies may be altered during brain maturation and could provide new insights into the disrupted thalamocortical organization in schizophrenia.

Here, we leveraged a cohort of individuals with early-onset schizophrenia (EOS), a disorder that is neurobiologically continuous with its adult counterpart,²⁹ to examine whether macroscale thalamic functional organization shows disturbances in the still developing brain of schizophrenia, mirroring neocortical reports. To this end, we first evaluated functional hierarchies of the thalamus by employing dimension reduction techniques on thalamocortical FC.³⁰ We then embedded thalamic functional hierarchies in a neurobiological context by spatially correlating the macroscale patterns with gene expression maps from the Allen Human Brain Atlas (AHBA).³¹ Last, we tested whether the functional hierarchies could estimate clinical symptoms of patients using a machine learning regression strategy.

Materials and Methods

Participants and Data Preprocessing

A total of 199 pediatric subjects (7–17 years) including 99 antipsychotic-naïve first-episode EOS patients and 100 typically developing (TD) controls were recruited from the First Hospital of Shanxi Medical University. See [Supplementary table S1](#) for demographic and clinical data. More details about the participants, MRI data acquisition, and preprocessing can be found in [Supplementary material](#).

Macroscale Thalamocortical Gradient Identification

Gradients of thalamocortical FC were generated to describe thalamic functional organization using the diffusion embedding algorithm in BrainSpace Toolbox.³² Thalamocortical functional connectivities were first calculated for each subject,^{19,26} and then converted into cosine similarity matrices.^{19,20} Subsequently, nonlinear dimensionality reduction techniques were employed on similarity matrices to resolve connectome gradient.³⁰ The relative positioning of thalamic voxels along each organizational axis describes similarity of their functional connectivity profiles. To quantify the dispersion of each thalamic voxel in the gradient space, we computed eccentricity, ie, the square root of the Euclidian distance from each thalamic voxel to the center of mass.³³ See [Supplementary material](#) for details. Additionally, we

explored cortical-thalamic gradients by generating cortical similarity matrices from cortical-thalamic connectivity profile ([Supplementary material](#)).

Thalamic Functional Network Division

To characterize the functional relevance of macroscale thalamic gradient space, we created a thalamic functional atlas including six large-scale functional networks: the visual (VIS), sensorimotor (SMN), dorsal attention (DAN), ventral attention (VAN), frontoparietal (FPN), and default mode (DMN) networks.³⁴ See [Supplementary material](#) for details. Except for dividing the thalamus into networks, we projected thalamic gradients onto the cerebral cortex and evaluated their correspondence with cortical functional networks ([Supplementary material](#)).

The Core-Matrix Cytoarchitecture

To delineate the core-matrix cytoarchitecture in the thalamus, we used the spatial maps of mRNA expression levels for two calcium-binding proteins (CALB1 and PVALB).⁸ Thalamic voxels with positive CP values (CALB1-PVALB values) related to areas with mostly matrix projection cells, and voxels with negative values related to regions mostly composed of core cells. CP map and between-group difference map of eccentricity were spatially correlated to investigate association between the thalamic cytoarchitecture and disturbed functional organization in EOS patients. Subsequently, we projected CP maps onto the cerebral cortex to investigate couplings between the core-matrix cytoarchitecture and FC. Cortical parcels with positive coupling values indicated as preferential associations with thalamic matrix cell populations, and negative values suggested associations with core cell populations. To evaluate cognitive terms associated with cytoarchitecture–connectome coupling maps, we further conducted topic-based behavioral decoding using NeuroSynth meta-analytic database.³⁵ See [Supplementary material](#) for details.

Clinical Correspondences

To investigate clinical significance of thalamic functional organization disturbances, we further associated the macroscale functional phenotype with schizophrenia-related gene expression. We selected out a number of protein-coding genes that were suggested to be particularly implicated in schizophrenia etiology or treatment ([Supplementary table S2](#))³⁶ and correlated their expression maps with between-group difference map of eccentricity. Second, we estimated the relationship between thalamic functional hierarchies and illness-related behaviors in EOS patients. Following a machine learning pipeline, we used eccentricity values to predict clinical symptoms in EOS.³⁷ See [Supplementary material](#) for detailed analyses.

Group Comparisons Between EOS and TD

Between-group differences on all kinds of measurements were assessed by using two-sample *t*-tests with covariates including age, gender, and head motion [mean frame-wise displacement, (FD)] (see [Supplementary material](#) for details).

Results

This study combined in vivo resting-state fMRI data, ex vivo thalamic cytoarchitectural approximations, meta-analytic database, and clinical behaviors, to determine macroscale thalamic functional organization abnormalities in EOS and their cytoarchitectural basis, cognitive, and clinical relevance ([figure 1](#)).

Macroscale Thalamic Gradients in TD and EOS

The principal gradient (G1, 30% explained) of the thalamus revealed a L–M axis, and the second gradient (G2, 14% explained) described an A–P axis, in line with previous work.²⁸ In [Supplementary figure S2](#), we also showed the third gradient pattern running in ventral-dorsal direction (9% explained). In EOS patients, we observed expansions at both anchors of the G1; the lateral portions including the ventral lateral and ventral posterior thalamic nuclei, the medial dorsal areas compared to TD controls ([figure 2A](#), threshold-free cluster enhancement (TFCE), $P < .005/2$). We also observed expansions along the G2 axis including the pulvinar and anterior nuclear groups ([figure 2B](#), TFCE, $P < .005/2$). Combining G1 and G2 axes, we computed an eccentricity score using the square root of the Euclidian distance from each thalamic voxel to the center of mass in the two-dimensional gradient space.³³ Global eccentricity was assessed for each participant by averaging eccentricity values across all thalamic voxels. We found significantly increased global eccentricity for thalamic voxels in EOS compared to TD ($t = 2.34$, $P = .02$), indicating a functional segregation of macroscale thalamic organization in patients ([figure 2C](#)). In line with thalamocortical gradient results, cortical-thalamic gradient axes were also extended in EOS ([figure S3](#) in [Supplementary material](#)).

Functional Relevance

Utilizing a whole-brain functional network parcellation,³⁴ thalamic voxels were distributed into six large-scale functional networks ([figure 3A](#)). For each subject, gradient loadings were averaged across voxels that were related to a certain network, and resulting network-level gradients were then compared between the EOS and TD groups ([figure 3B](#), Bonferroni correction, $P < .05/6$). EOS patients had significantly higher mean G1 scores in the SMN ($t = 5.37$, $P < .0001$) and DAN ($t = 2.94$, $P = .004$). Besides, patients had significantly lower G1 scores in the

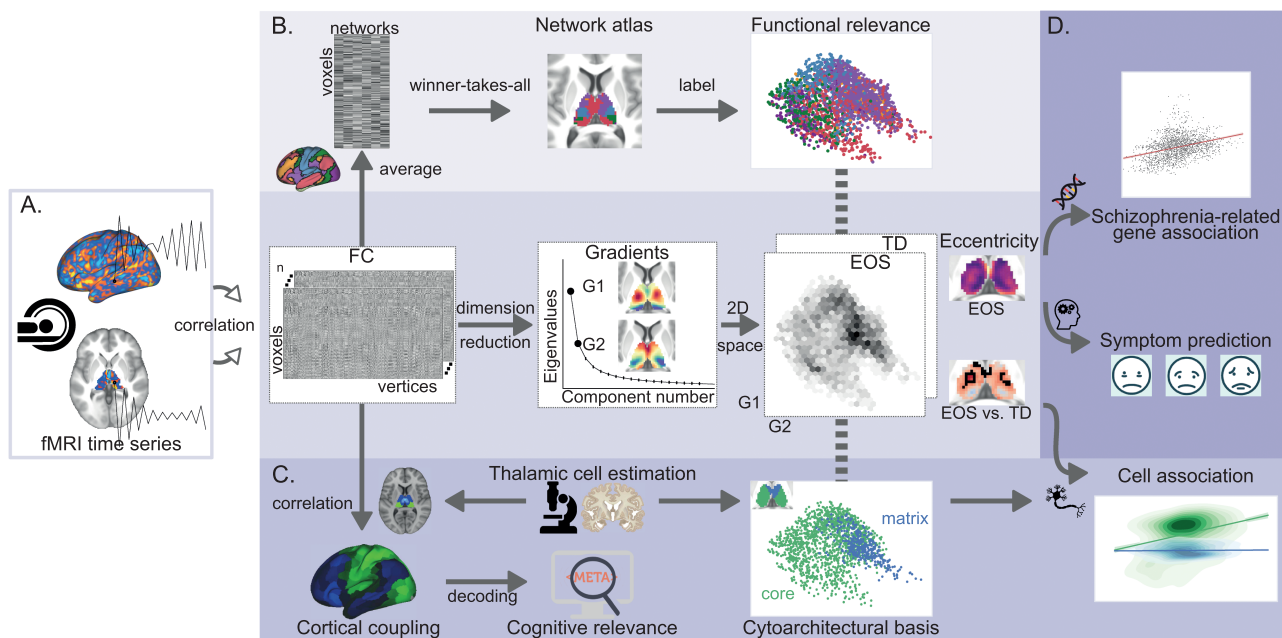


Fig. 1. Study overview. (A) Macroscale thalamocortical gradients identification. Gradients were computed by employing a dimension reduction method on thalamic voxels \times cortical vertices functional connectome (FC) matrices for all subjects ($n = 177$). Two-dimensional (2D) gradient spaces were then constructed by combining the first gradient (G1) and the second gradient (G2). Eccentricity values were defined as the square root of the Euclidian distance from each thalamic voxel to the center of mass in the 2D space. Group comparisons [t -tests, early-onset schizophrenia (EOS) vs typically developing (TD)] were separately employed on G1, G2, and eccentricity. (B) Thalamic functional network division. Voxels \times vertices FC matrices were column-wise averaged according to a cortical functional network atlas, and resulting voxels \times networks matrices were then averaged across subjects. Each thalamic voxel was labeled by the network showing the highest correlation with it, thereby generating a network atlas for the thalamus. (C) The core-matrix cytoarchitectural basis. Thalamic core and matrix cell distributions were estimated by mRNA expressions of PVALB and CALB1, respectively. The matrix vs core relative distribution (CALB1-PVALB expression values) in the thalamus was spatially correlated with thalamus \times cortex FC matrices to create cytoarchitecture-connectome couplings in the cortex, which were further used for cognitive decoding. Additionally, spatial correlations were employed between the matrix vs core relative distribution and between-group difference map of eccentricity. (D) Clinical correspondences. For EOS patients, their eccentricity maps were first spatially correlated with schizophrenia-related gene expression maps, and were then used to predict several symptom domains based on a linear regression model.

VAN ($t = -2.85$, $P = .005$), FPN ($t = -3.69$, $P = .0003$), and DMN ($t = -3.03$, $P = .003$) relative to TD controls. For the G2 axis, patients showed decreased gradient scores in the VIS ($t = -4.08$, $P < .0001$), and increased in the DMN ($t = 5.45$, $P < .0001$). In the two-dimensional gradient space showing functional relevance (figure 3C), EOS patients had apparent dissociation of SMN-related thalamic voxels along the G1 axis. Dissociation of these voxels indicates their functional connectivity profiles are less similar with that of other voxels, suggesting a functional segregation. Along the G2 axis, patients showed a larger functional segregation between VIS- and DMN-related regions. Cortical projections of thalamic gradients further validated the functional relevance (figure S4 in Supplementary material).

The Core-Matrix Cytoarchitectural Basis

Having established macroscale thalamic connectome gradients, we further investigated whether connectome differences between patients and controls were specific to

thalamic cytoarchitectural features, namely core vs matrix cells, motivated by a previous work.⁸ The differential expression level between CALB1 and PVALB, ie, CP scores, was used to delineate thalamic core-matrix type cell distribution, where positive/negative CP value corresponded to preferentially matrix/core cell population, respectively (figure S5 in Supplementary material). We then mapped the core-matrix cytoarchitectural features onto the two-dimensional gradient space (figure 4A). Core cells showed mildly increased global eccentricity in EOS patients compared with core cells of TD ($t = 2.38$, $P = .02$), but matrix cells did not ($t = 1.62$, $P = 0.11$). No significant difference was found between global eccentricity of core and matrix populations within EOS ($t = 1.07$, $P = .29$) or TD ($t = 0.36$, $P = 0.72$). A negative spatial correlation was found between CP values and t values of eccentricity (figure 4B, $r = -.29$, $P_{\text{vario}} = .002$). In detail, increased dispersion of macroscale connectome gradient space in patients was particularly related to core cells ($r = .31$, $P_{\text{vario}} < .0001$), rather than matrix cells ($r = .02$, $P_{\text{vario}} = .84$).

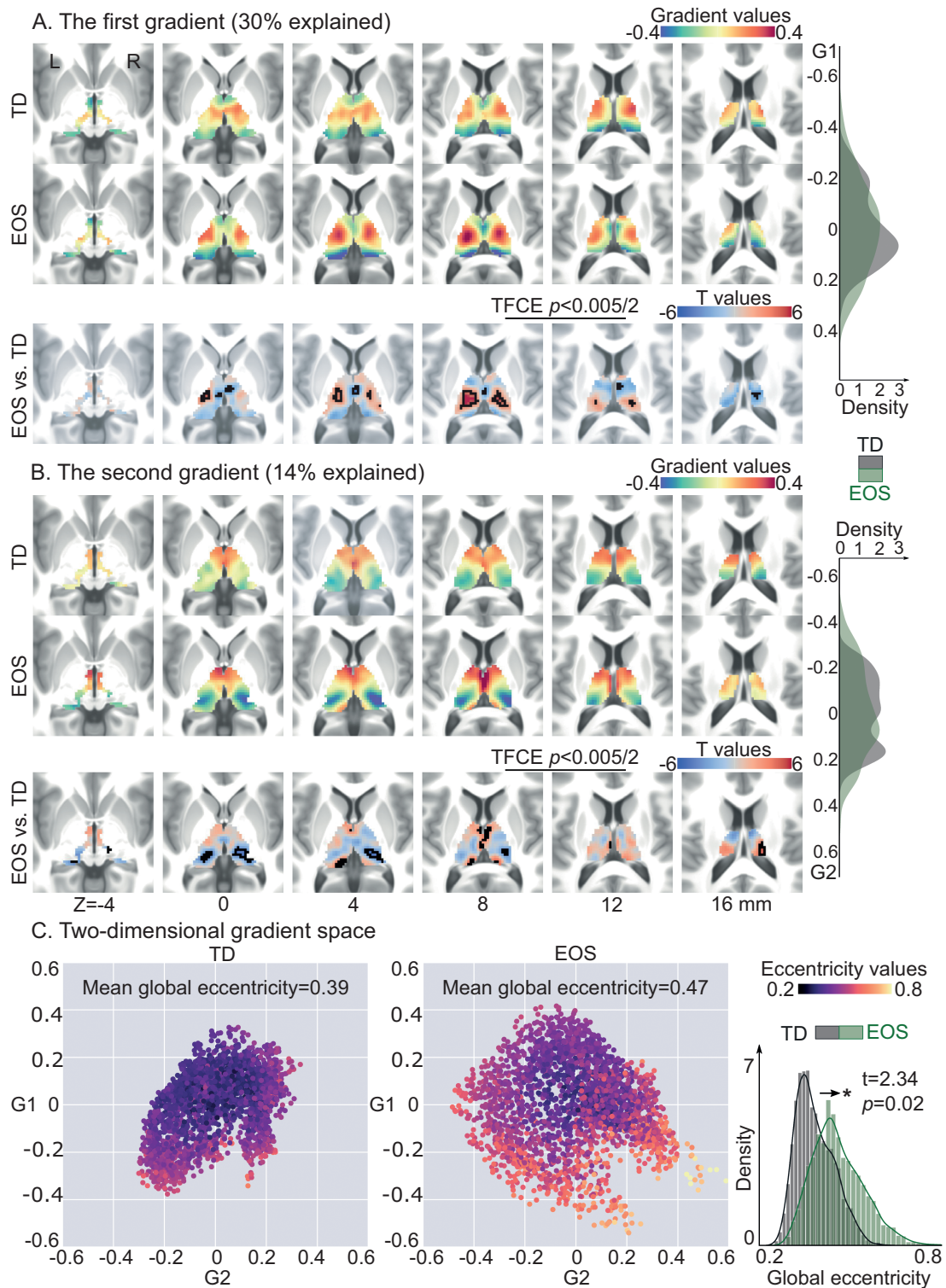
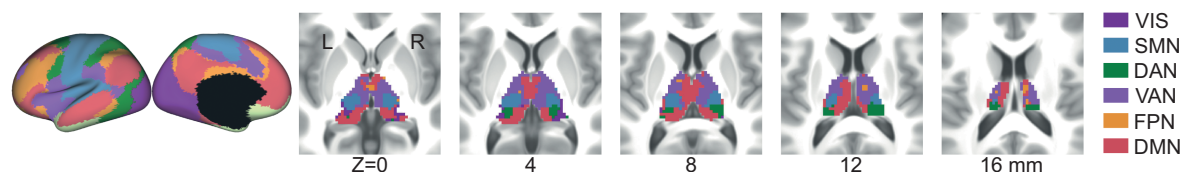
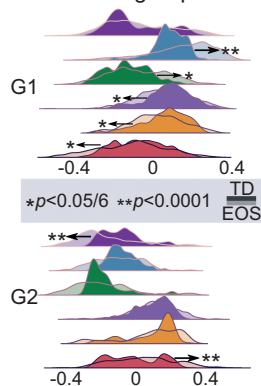


Fig. 2. Thalamic gradients in TD controls and EOS patients. (A) The group-level G1 for TD and EOS, and their between-group differences. The G1 depicts a transition from lateral to medial portions of the thalamus. Thalamic voxels showing significant G1 score differences were surrounded by black contours [*t*-test, EOS vs TD; threshold-free cluster enhancement (TFCE), $P < .005/2$]. The density map plotted by kernel density estimation function represents the distribution of G1 loading for EOS or TD. The density value is related to the count of thalamic voxels falling within a certain gradient bin. (B) The group-level G2 for TD and EOS, and their differences. G2 separates the anterior thalamic portions from the posterior portions. Thalamic voxels with significant G2 differences were surrounded by black contours. The density map represents the G2 loading for EOS or TD. (C) Gradient spaces built on the group-level G1 and G2, separately for TD and EOS. Each point represents a thalamic voxel embedded in the gradient space. Voxels are color coded based on their mean eccentricity scores across subjects. Higher eccentricity indicates greater segregation, eg, larger dissimilarity of thalamocortical connectivity, in the gradient space. The density plot depicts the distribution of eccentricity scores in EOS and TD.

A. Functional atlas of the thalamus



B. Between-group differences



C. Two-dimensional gradient space with functional networks

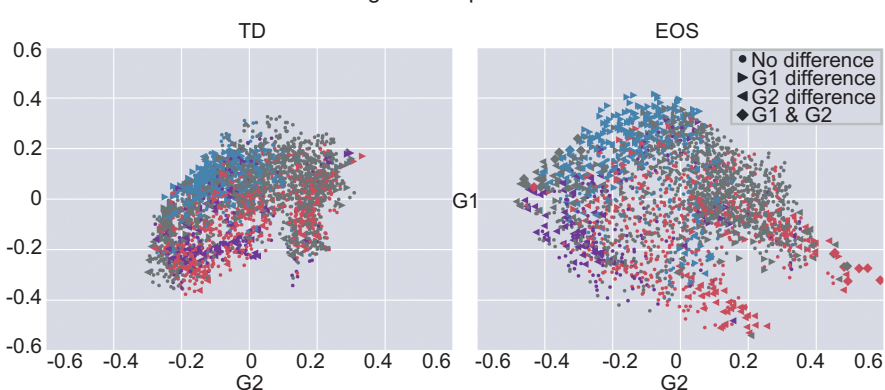


Fig. 3. Thalamic gradients distributed into functional networks. (A) Network-level representations of the thalamocortical connectome. (B) G1 and G2 scores within functional networks. Density maps indicate gradient scores (top: G1, bottom: G2) within six networks for EOS and TD. Network-level differences between EOS and TD were accessed by t-tests, and significant differences are depicted by * (Bonferroni correction, $P < .05$) and ** ($P < .0001$). (C) Gradient space representation of the thalamus together with functional networks for TD (left) and EOS (right). Thalamic voxels are situated based on their G1 (x -axis) and G2 (y -axis) scores, and are colored according to their network assignment. Filled point right stands for the G1 score differences between EOS and TD; filled point left for the G2 score differences; filled diamond for both G1 and G2 score differences; filled circle for no difference. VIS, the visual network; SMN, the sensorimotor network; DAN, the dorsal attention network; VAN, the ventral attention network; FPN, the frontoparietal network; DMN, the default mode network.

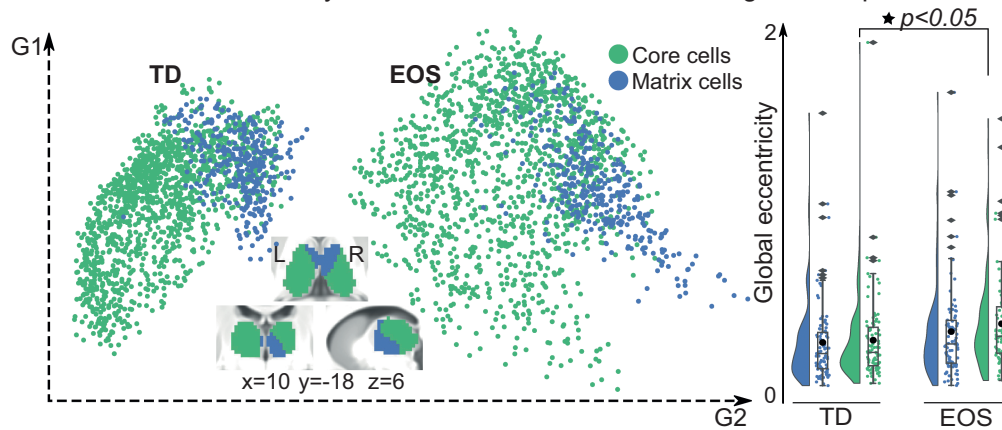
Given the association between CP map and thalamo-cortical connectome, we further assessed whether cytoarchitecture-connectome coupling contributes to cognitive processing. Thus, we projected the core-matrix cytoarchitecture to the cerebral cortex and then conducted a behavioral decoding using the NeuroSynth database.³⁵ Core cell populations were mainly associated with unimodal regions, and matrix cell populations were associated with transmodal cortices (figure S6 in Supplementary material). Compared with TD controls, EOS patients showed increased cytoarchitecture-connectome coupling, ie, closer associations with matrix cells in the DMN and FPN (figure 4C, FDR, $P < .005$). These abnormal coupling increases were associated with seven cognitive topics including declarative memory, autobiographical memory, working memory, verbal semantics, social cognition, language, and visuospatial (z -statistic > 3.1), indicating its implications in higher-level cognitive processes. Additionally, reduced cytoarchitecture-connectome coupling, ie, more preferential associations with core cells were observed in the VIS, DAN, and SMN. These reductions were characterized by low-level visual sensory and motor functions involving visual perception, visual attention, motor, action, eye movements, visuospatial, multisensory processing, and reading (figure 4D).

Clinical Relevance

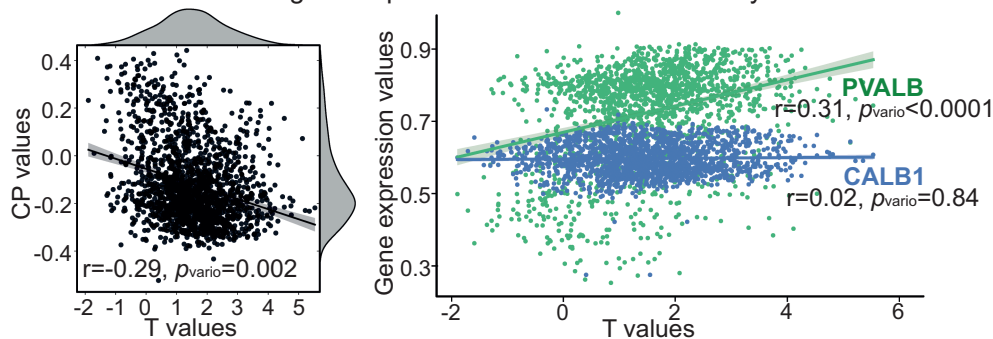
To reveal clinical significance of the macroscale functional gradients, we first explored its associations with schizophrenia-related gene expression maps, based on a previous work³⁶ (figure 5A). The difference map of eccentricity scores between patients and controls was significantly correlated with mRNA expression levels for Glutamatergic neurotransmission-related genes including GRIN2A ($r = .34$, $P_{\text{vario}} = .001$), GRIA1 ($r = -.23$, $P_{\text{vario}} = .03$), calcium signaling-related genes RIMS1 ($r = .26$, $P_{\text{vario}} = .005$), synaptic function and plasticity-related genes including CNTN4 ($r = .32$, $P_{\text{vario}} = .001$) and SNAP91 ($r = .24$, $P_{\text{vario}} = .02$), other neuronal ion channels-related genes including HCN1 ($r = .25$, $P_{\text{vario}} = .03$) and CHRNA5 ($r = .33$, $P_{\text{vario}} = .001$), neurodevelopment-related genes including BCL11B ($r = -.23$, $P_{\text{vario}} = .02$) and FAM5B ($r = .27$, $P_{\text{vario}} = .006$). No significant correlation was observed in the other 19 genes, including therapeutic target-related genes.

Second, we investigated whether thalamic gradients could predict clinical symptoms in EOS. We used eccentricity scores as input features in a linear regression model to estimate patients' positive and negative scores of the Positive and Negative Syndrome Scale (PANSS) (figure S7). Eccentricity scores of thalamic voxels

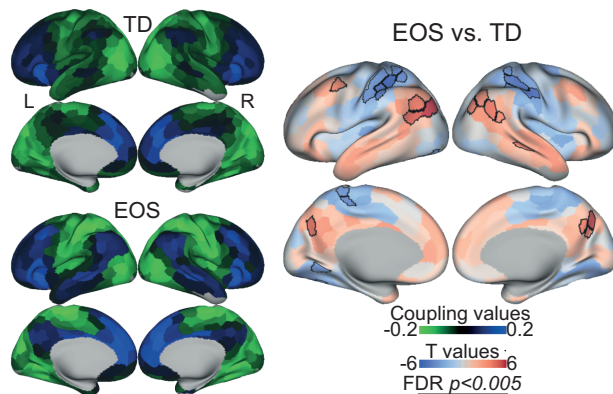
A. Thalamic Core-Matrix cytoarchitecture in two-dimensional gradient space



B. Associations between gene expression levels and eccentricity abnormalities



C. Gene-connectome coupling abnormalities



D. Cognitive topics-decoding

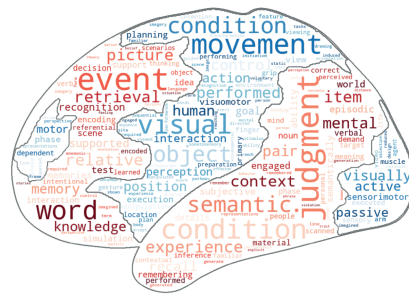
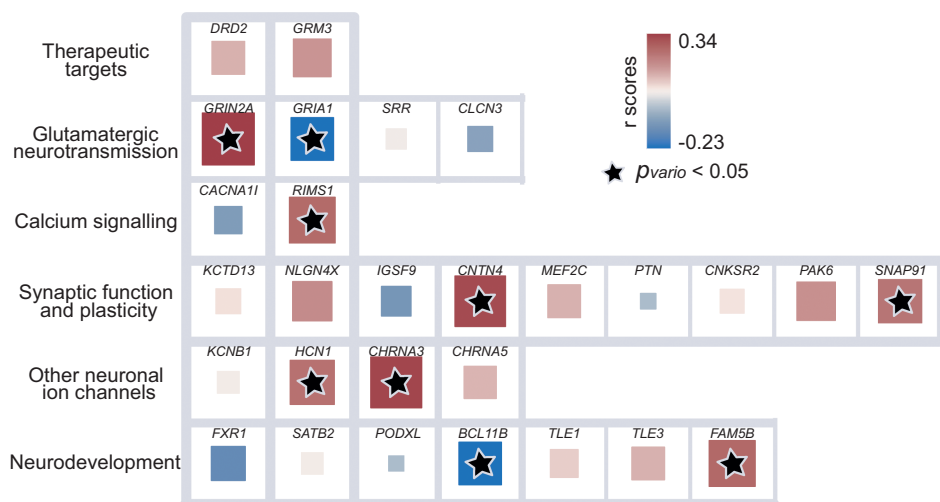
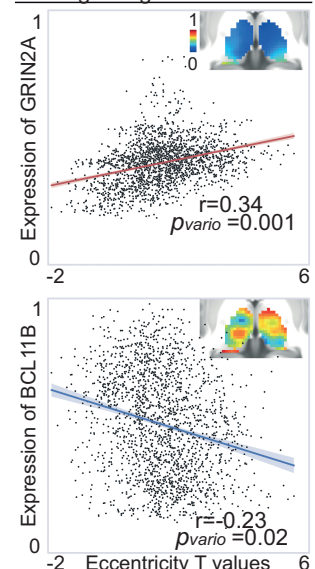


Fig. 4. The core-matrix cytoarchitecture of the thalamus. (A) Core-matrix cytoarchitectural features of thalamic voxels projected onto the two-dimensional gradient space for TD and EOS. Rainclouds present group comparisons of global eccentricity in four fashions: global eccentricity values across core cells in EOS vs global eccentricity values across matrix cells in EOS; core cells in TD vs matrix cells in TD; core cells in EOS vs core cells in TD; matrix cells in EOS vs matrix cells in TD. Filled star represents P value $< .05$. (B) Associations between eccentricity differences (t values; EOS vs TD) and CALB1-PVALB expression levels (CP values, left) as well as CALB1 and PVALB expression levels (right). Correlations were obtained across thalamic voxels (Pearson r values) and their statistical significances were tested using the variogram methods that control for the spatial autocorrelations (P_{vario} values). (C) Parcel-wise couplings between FC and cytoarchitecture for TD and EOS, and their differences (t -test, EOS vs TD). Cortical parcels with positive coupling values indicate as preferential associations with matrix thalamic cells, and negative coupling values suggested core cells. Parcels with significantly different coupling patterns in patients are surrounded by black contours [false discovery rate (FDR), $P < .005$]. (D) Topic-based behavioral decoding of regions with abnormal couplings in EOS. Cognitive terms in warm color correspond to brain regions showing hyper-couplings in patients relative to controls, and cool color represent hypo-couplings. In the word cloud, the size of a cognitive term is proportional to its loading strength for decoding an input brain mask.

A. Correlations with 28 schizophrenia-related gene expressions



Two highest gene correlations



B. Predicting clinical symptoms by eccentricity maps in EOS

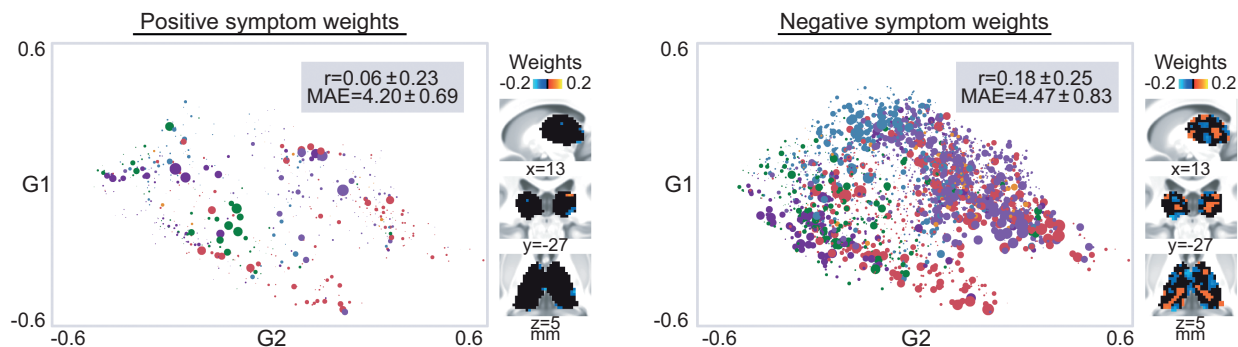


Fig. 5. Clinical relevance of thalamic gradients in EOS. (A) The relationship between the macroscale functional phenotype and schizophrenia-related gene expressions. Interregional correlations (Pearson r values) were employed between eccentricity differences (t values; EOS vs TD) and gene expression levels, and their significances were evaluated by variogram approach (filled star represents $P_{\text{vario}} < .05$). In the left panel, the size of a square is in proportion to absolute value of corresponding Pearson r coefficient, and its color is coded by the sign of r value. The highest positive correlation (top right) with eccentricity differences was found at a glutamatergic neurotransmission protein-coding gene, ie, GRIN2A, whose gene expression pattern in the thalamus is shown on the top right corner. The highest negative correlation (bottom right) was found at BCL11B, a neurodevelopment-related gene. (B) The relationship between thalamic functional organization and clinical presentations. Eccentricity values in patients were used to predict PANSS positive and negative scores based on a linear regression model. Pearson r coefficients, and mean absolute error (MAE) between observed and predicted clinical scores were calculated to evaluate the model performance. The optimal model parameter (L1 ratio) was 0.3 for positive symptoms prediction and 0.1 for negative symptoms, leading to less predictive voxels for positive symptom (points in the left graph) than negative symptom (points in the right graph). This procedure including model learning and testing was repeated 100 times, generating the distributions of r coefficients and MAE. Absolute value of mean feature coefficients across 100 models was used as weight for each thalamic voxel (a point). The size is coded by predictive weight, and is colored according to its network assignment.

performed moderately when predicting the severity of negative symptoms ($r = .18 \pm .25$, $\text{MAE} = 4.47 \pm 0.83$), while poor in the prediction of positive symptoms ($r = .06 \pm .23$, $\text{MAE} = 4.20 \pm 0.69$). For positive and negative symptoms, mean predictive weights across 100 fitted models were separately reported in figure 5B. In the model predicting negative symptoms, weights were heavier in the thalamic voxels regarding to transmodal networks such as the VAN and DMN.

Discussion

In the current study we investigated macroscale thalamic functional organization in EOS through dimensionality reduction techniques on thalamocortical functional connectivity. We found both expansions along L–M principal axis and A–P secondary axis of thalamic hierarchies in EOS, indicating connectivity profiles between both anchors showed higher dissimilarities in patients versus controls. Disordered functional hierarchies of the thalamus

were related to altered thalamocortical interactions both in unimodal and transmodal networks. To evaluate the cytoarchitectural underpinnings of the macroscale functional organization disturbances in EOS, we compared alterations in functional organization within core and matrix cells that derived from an independent transcriptomic atlas. We found that in particular, functional organization related to thalamic core cells was altered in EOS. Patients' abnormal coupling patterns between a-priori map of the core-matrix cytoarchitecture and FC characterized a spectrum from perceptual to abstract cognitive functions. Moreover, transcriptomic-informed analyses suggested a close relationship between macroscale functional organization and schizophrenia etiology-related gene expressions in the thalamus. Employing a machine learning strategy, we found that thalamic functional organization was able to predict negative symptoms in EOS. In sum, the current findings provide mechanistic evidence for disrupted thalamocortical system in EOS, and point to alterations in functional networks associated with both perceptual and cognitive functions, suggesting a unitary pathophysiology of heterogeneous symptoms in schizophrenia.

In line with previous work on thalamic hierarchies,²⁸ the principal functional gradient described continuous transition from the ventral lateral nucleus to the anterior and pulvinar groups, and the second axis delineated gradual transition from the anterior nuclei to the pulvinar. Whereas L–M thalamic axis has been reported to correspond to the distribution of gray matter morphology, ie, low-to-high intensity of neural mass, and the A–P gradient was strongly related to the intrinsic geometry of the thalamus. These findings suggested an association between functional thalamic hierarchies and its structure. Albeit not directly shown, L–M and A–P axes may reflect functional relevance in different dimensions, ie, two kinds of transitions across functional networks. Indeed, we found that the L–M principal axis functionally segregated the VIS and SMN, similar to the second gradient of cortical connectome.¹⁹ Conversely, the A–P axis of thalamic hierarchies segregated unimodal and transmodal networks, in accord with previous findings.²⁸ Taken together, beyond supporting macroscale thalamic hierarchical framework, the current findings further broaden our knowledge of functional specialization of thalamic L–M and A–P axes.

Thalamic ventral lateral and ventral posterior nuclei, as one end of the L–M organizational axis, exhibited evident dissociation in EOS. Both nuclei receive neuronal input from the sensory periphery, and project to the motor and somatosensory cortices, respectively.³⁸ The etiology of schizophrenia has been suggested to damage refinement of motor/somatosensory-thalamic connectivity patterns that occurs during brain maturation.¹⁷ Indeed, in adolescent patients relative to adult patients, structural abnormalities in the sensorimotor cortex are reported

to be particularly salient,³⁹ but may gradually fade out within a longitudinal period of observation.⁴⁰ Moreover, motor performance has been reported worse in adolescent patients relative to adult patients when accounting for developmental factors.⁴¹ In line with this observation, a meta-analysis suggested that motor deficits may precede the onset of schizophrenia and may constitute robust antecedents of this mental disorder.⁴² In the context, we postulate sensorimotor-related segregation along thalamic L–M hierarchy might underlie premorbid disturbances in motor development, a marker distinct to schizophrenia.

Compared with TD, EOS patients had increased segregation in two extremes of the A–P axis, ie, visual-related pulvinar nucleus and default mode-associated anterior nuclear group. Weaker functional connectivity between the VIS and DMN has been previously reported in EOS.^{43,44} In fact, given the central role of the thalamus in the development of the cerebral cortex,¹¹ abnormalities of the cerebral cortex in schizophrenia might occur secondary to thalamic pathology.^{4,45} Thus, the unimodal–transmodal thalamic hierarchy expansion might further result in disturbed cortical differentiation of unimodal and transmodal regions in EOS. A compression of the unimodal-to-transmodal cortical hierarchy was recently found in chronic adult-onset schizophrenia,⁴⁶ contrasting with our observation of cortical-thalamic hierarchy expansion. Given age-dependent shifts in the macroscale cortical hierarchy,⁴⁷ this inconsistency might due to their disparate stage of the illness and age of onset, or their usage of antipsychotic drugs. Notably, we could not rule out another possible reason that EOS and adult-onset schizophrenia are different disease entities with divergent development trajectories. Etiologically, EOS appears to have greater genetic salience than its relatively heterogeneous adult counterpart confounded by environmental factors,⁴⁸ laying a foundation for this possibility. Despite mounting studies indicate EOS as an early and severe variant of adult-onset schizophrenia,^{49,50} the hypothesis of different disease entities should still be considered. Further longitudinal works are needed to chart functional organization abnormalities of the thalamus and the cerebral cortex during the course of schizophrenia. Nevertheless, the current findings embed thalamus into a cortical functional organization linked to differentiation of sensory from abstract cognitive functions, paving the way to comprehensively reveal cognitive defects, another well documented precursor of schizophrenia excepts for motor deficits.⁴²

Leveraging our observations of alterations of thalamic functional organization against a proxy map of core/matrix cells based on postmortem transcriptomic data,⁸ we observed thalamic core cells to underlie expansive functional hierarchies in EOS, rather than matrix cells. Core and matrix cells are two primary types of thalamic relay neurons which separately exhibit immunoreactivity to the

calcium-binding proteins Parvalbumin and Calbindin.⁹ Thalamic nuclei differ in the ratio of core and matrix neurons.⁵¹ Specifically, sensory and motor relay nuclei, as well as the pulvinar nuclei and the intralaminar nuclei are chiefly composed of core cells.⁵² Compared with matrix cells, core cells innervate middle cortical layers in a more area-restricted and topographically-organized fashion.⁹ Functionally, Parvalbumin-rich core cells have been reported to act as drivers of feedforward activity, while Calbindin-rich matrix cells fulfill a more modulatory function.⁷ Together, this may suggest that thalamic hierarchy disturbances in EOS may relate to the “feed-forward” pathway that transmits information from the sensory periphery, not the “feed-back” pathway.⁵³

A further inspection of cytoarchitecture–connectome coupling abnormalities in EOS by evaluating the selective connection of the core-matrix cytoarchitecture with the cortex could show that, patients’ core thalamus dysconnected with both unimodal and transmodal cortices. In healthy adults, core regions have preferential projections with unimodal primary regions, and matrix areas with transmodal cortices incorporating the DMN, FPN, VAN and the limbic network.⁸ Conversely in the current pediatric sample, we observed core-related connections with both unimodal and posterior transmodal cortices for TD, whereas EOS had larger similarity with the previously reported adult pattern, ie, stronger core-related couplings in the VIS, SMN and DAN and weaker core-related couplings in the DMN and FPN. To some extent, these cytoarchitecture–connectome coupling abnormalities account for previous findings of thalamo-prefrontal and thalamo-sensorimotor dysconnectivity in EOS.^{13,14} Weaker core-related coupling in the prefrontal regions relates to thalamo-prefrontal hypoconnectivity, and stronger core-related coupling in the sensorimotor regions relates to thalamo-sensorimotor hyperconnectivity. Therefore, core-related coupling abnormalities in EOS may imply a shared pathophysiological mechanism of dysconnectivity as previously suggested.¹⁸ Together, our results imply putatively excessive maturation in the thalamocortical feedforward pathway of schizophrenia. However, future molecular-level work is undoubtedly needed to elaborate on the feedforward pathway alterations in the still developing brain of schizophrenia.

It has been suggested that schizophrenic brain may not form connections according to gene encoded blueprints which have been phylogenetically determined to be the most efficient.⁵⁴ In line with this, we observed that impaired thalamic hierarchy in EOS was highly associated with schizophrenia-related gene expressions, especially genes encoding Glutamatergic neurotransmission and neurodevelopmental proteins.³⁶ Our findings reveal a gene-connectome correspondence in the thalamocortical system of EOS, adding new evidence for genetics of schizophrenia. However, there is an obvious shortage in our gene-related analyses. The gene expression levels

were assessed from postmortem brain tissue of adults,³¹ which might be different from the pediatric human brain. Limited by the lack of pediatric transcriptional atlas, our findings about the association between macroscale connectome topology and genetic architecture should be carefully considered.

Behavioral decoding of the cytoarchitecture–connectome coupling pattern derived a sensory-cognitive architecture, describing functions associated with primary sensory and multisensory processing to working memory, cognitive control and motivation. Along the continuous behavioral spectrum, perception (especially visual sensory), motor, and higher cognition such as memory are particularly affected by schizophrenia. Consistently, thalamic hierarchy abnormalities were sensorimotor-related, as well as visual/ default mode-associated along a second axis. As the “cognitive dysmetria” theory suggested, the multitude and diversity of behavior deficits in schizophrenia might be tied to an impaired fundamental cognitive process mediated by the thalamus.^{54,55} This impairment, ie, cognitive dysmetria referred to a disruption of the fluid and coordinated sequences of both thought and action, leading to a decreased coordination of perception, retention, retrieval, and response functions.⁵⁶ In particular, our study suggested that abnormal thalamic hierarchy was closely related to negative symptoms of schizophrenia, ie, a diminution of functions related to motivation and interest. Compared to positive symptoms (such as delusions), negative symptoms are more complex and likely to be the result of systematic disruption. Effective treatment of negative symptoms has long been a clinical challenge for its poor outcomes. The current study provides a thalamic hierarchy framework for heterogeneous behavior deficits related to negative symptoms in schizophrenia, which might denote future therapy of the resistant symptoms.

In sum, the current study describes thalamic functional organization abnormalities in EOS, which could be related to “feed-forward” core thalamocortical pathway. The macroscale disruptions were related to schizophrenia-related genetic factors. Crucially, it might perturb behaviors involving both low-level perception and high-level cognition, resulting in diverse negative syndromes in schizophrenia.

Supplementary Material

Supplementary material is available at <https://academic.oup.com/schizophreniabulletin/>.

Acknowledgments

We are grateful to all the participants and their guardians in this study. This work was supported by the National Natural Science Foundation of China (82121003, 62036003, 62073058, 62173070), Innovation Team and

Talents Cultivation Program of National Administration of Traditional Chinese Medicine (ZYXCXTD-D-202003). S.L.V. was also funded in part by Helmholtz Association's Initiative and Networking Fund under the Helmholtz International Lab grant agreement InterLabs-0015, and the Canada First Research Excellence Fund (CFREF Competition 2, 2015-2016) awarded to the Healthy Brains, Healthy Lives initiative at McGill University, through the Helmholtz International BigBrain Analytics and Learning Laboratory (HIBALL).

Conflict of interest statement: This is an original manuscript and no part of this manuscript is being considered for publication elsewhere. The data that support the findings of this study are available from the corresponding author upon reasonable request. All authors have approved this manuscript. The authors declare that they have no conflict of interest.

Data and Code Availability

The data that support our findings are available from the corresponding author upon reasonable request. The estimated spatial maps of mRNA expression levels were downloaded at: <https://www.meduniwien.ac.at/neuroimaging/mRNA.html>. The code for functional gradient analysis was adapted from the MICA lab (<http://mica-mni.github.io>) and is available at <https://github.com/Yun-Shuang/Thalamic-functional-gradient-SZ>. The code for behavioral decoding was adapted from https://github.com/NeuroanatomyAndConnectivity/gradient_analysis. Statistical analyses were carried out using PALM (<https://fsl.fmrib.ox.ac.uk/fsl/fslwiki/PALM>) and BrainSMASH (<https://brainsmash.readthedocs.io/en/latest/>). Machine learning analyses were based on scikit-learn package (https://scikit-learn.org/stable/modules/generated/sklearn.linear_model.ElasticNetCV). Results were visualized using Connectome Workbench (<https://www.humanconnectome.org/software/connectome-workbench>), and Seaborn (<https://seaborn.pydata.org/>) in combination with ColorBrewer (<https://github.com/scottclowe/cbrewer2>).

References

- Kinney DK, Matthyse S. Genetic transmission of schizophrenia. *Annu Rev Med*. 1978;29:459–473.
- Stephan KE, Friston KJ, Frith CD. Dysconnection in schizophrenia: from abnormal synaptic plasticity to failures of self-monitoring. *Schizophr Bull*. 2009;35(3):509–527.
- Shine JM. The thalamus integrates the macrosystems of the brain to facilitate complex, adaptive brain network dynamics. *Prog Neurobiol*. 2021;199:101951.
- Jones EG. Cortical development and thalamic pathology in schizophrenia. *Schizophr Bull*. 1997;23(3):483–501.
- Pergola G, Selvaggi P, Trizio S, Bertolino A, Blasi G. The role of the thalamus in schizophrenia from a neuroimaging perspective. *Neurosci Biobehav Rev*. 2015;54:57–75.
- Jones EG. Synchrony in the interconnected circuitry of the thalamus and cerebral cortex. *Ann N Y Acad Sci*. 2009;1157:10–23.
- Jones EG. The thalamic matrix and thalamocortical synchrony. *Trends Neurosci*. 2001;24(10):595–601.
- Muller EJ, Munn B, Hearne LJ, et al. Core and matrix thalamic sub-populations relate to spatio-temporal cortical connectivity gradients. *Neuroimage*. 2020;222:117224.
- Jones EG. Viewpoint: the core and matrix of thalamic organization. *Neuroscience*. 1998;85(2):331–345.
- Hwang K, Bertolero MA, Liu WB, D'Esposito M. The human thalamus is an integrative hub for functional brain networks. *J Neurosci*. 2017;37(23):5594–5607.
- Lopez-Bendito G, Molnar Z. Thalamocortical development: how are we going to get there? *Nat Rev Neurosci*. 2003;4(4):276–289.
- Nakagawa Y. Development of the thalamus: from early patterning to regulation of cortical functions. *Wiley Interdiscip Rev Dev Biol*. 2019;8(5):e345.
- Zhang M, Palaniyappan L, Deng M, et al. Abnormal thalamocortical circuit in adolescents with early-onset schizophrenia. *J Am Acad Child Adolesc Psychiatry*. 2021;60(4):479–489.
- Fryer SL, Ferri JM, Roach BJ, et al. Thalamic dysconnectivity in the psychosis risk syndrome and early illness schizophrenia. *Psychol Med*. 2022;52(13):2767–2775.
- Ferri J, Ford JM, Roach BJ, et al. Resting-state thalamic dysconnectivity in schizophrenia and relationships with symptoms. *Psychol Med*. 2018;48(15):2492–2499.
- Ramsay IS, Mueller B, Ma Y, Shen C, Sponheim SR. Thalamocortical connectivity and its relationship with symptoms and cognition across the psychosis continuum. *Psychol Med*. 2022;1:10.
- Woodward ND, Karbasforoushan H, Heckers S. Thalamocortical dysconnectivity in schizophrenia. *Am J Psychiatry*. 2012;169(10):1092–1099.
- Woodward ND, Heckers S. Mapping thalamocortical functional connectivity in chronic and early stages of psychotic disorders. *Biol Psychiatry*. 2016;79(12):1016–1025.
- Margulies DS, Ghosh SS, Goulas A, et al. Situating the default-mode network along a principal gradient of macroscale cortical organization. *Proc Natl Acad Sci USA*. 2016;113(44):12574–12579.
- Paquola C, Vos De Wael R, Wagstyl K, et al. Microstructural and functional gradients are increasingly dissociated in transmodal cortices. *PLoS Biol*. 2019;17(5):e3000284.
- Hong SJ, Vos de Wael R, Bethlehem RAI, et al. Atypical functional connectome hierarchy in autism. *Nat Commun*. 2019;10(1):1022.
- Vazquez-Rodriguez B, Suarez LE, Markello RD, et al. Gradients of structure-function tethering across neocortex. *Proc Natl Acad Sci USA*. 2019;116(42):21219–21227.
- Huntenburg JM, Bazin PL, Margulies DS. Large-scale gradients in human cortical organization. *Trends Cogn Sci*. 2018;22(1):21–31.
- Valk SL, Xu T, Paquola C, et al. Genetic and phylogenetic uncoupling of structure and function in human transmodal cortex. *Nat Commun*. 2022;13(1):2341.
- Bayrak S, Khalil AA, Villringer K, et al. The impact of ischemic stroke on connectivity gradients. *Neuroimage Clin*. 2019;24:101947.
- Meng Y, Yang S, Chen H, et al. Systematically disrupted functional gradient of the cortical connectome in generalized epilepsy: initial discovery and independent sample replication. *Neuroimage*. 2021;230:117831.

27. Dong D, Luo C, Guell X, *et al.* Compression of cerebellar functional gradients in schizophrenia. *Schizophr Bull.* 2020;46(5):1282–1295.
28. Yang S, Meng Y, Li J, *et al.* The thalamic functional gradient and its relationship to structural basis and cognitive relevance. *Neuroimage.* 2020;218:116960.
29. Jacobsen LK, Rapoport JL. Research update: childhood-onset schizophrenia: implications of clinical and neurobiological research. *J Child Psychol Psychiatry.* 1998;39(1):101–113.
30. Coifman RR, Lafon S. Diffusion maps. *Appl Comput Harmon Anal.* 2006;21(1):5–30.
31. Hawrylycz MJ, Lein ES, Guillozet-Bongaarts AL, *et al.* An anatomically comprehensive atlas of the adult human brain transcriptome. *Nature.* 2012;489(7416):391–399.
32. Vos de Wael R, Benkarim O, Paquola C, *et al.* BrainSpace: a toolbox for the analysis of macroscale gradients in neuroimaging and connectomics datasets. *Commun Biol.* 2020;3(1):103.
33. Park BY, Bethlehem RA, Paquola C, *et al.* An expanding manifold in transmodal regions characterizes adolescent re-configuration of structural connectome organization. *Elife.* 2021;10:e64694.
34. Yeo BT, Krienen FM, Sepulcre J, *et al.* The organization of the human cerebral cortex estimated by intrinsic functional connectivity. *J Neurophysiol.* 2011;106(3):1125–1165.
35. Yarkoni T, Poldrack RA, Nichols TE, Van Essen DC, Wager TD. Large-scale automated synthesis of human functional neuroimaging data. *Nat Methods.* 2011;8(8):665–670.
36. Schizophrenia Working Group of the Psychiatric Genomics C. Biological insights from 108 schizophrenia-associated genetic loci. *Nature.* 2014;511(7510):421–427.
37. Pedregosa F, Varoquaux G, Gramfort A, *et al.* Scikit-learn: machine learning in Python. *J Mach Learn Res.* 2011;12:2825–2830.
38. Ramcharan EJ, Gnadt JW, Sherman SM. Higher-order thalamic relays burst more than first-order relays. *Proc Natl Acad Sci USA.* 2005;102(34):12236–12241.
39. Douaud G, Smith S, Jenkinson M, *et al.* Anatomically related grey and white matter abnormalities in adolescent-onset schizophrenia. *Brain.* 2007;130(Pt 9):2375–2386.
40. Douaud G, Mackay C, Andersson J, *et al.* Schizophrenia delays and alters maturation of the brain in adolescence. *Brain.* 2009;132(Pt 9):2437–2448.
41. White T, Ho BC, Ward J, O’Leary D, Andreasen NC. Neuropsychological performance in first-episode adolescents with schizophrenia: a comparison with first-episode adults and adolescent control subjects. *Biol Psychiatry.* 2006;60(5):463–471.
42. Dickson H, Laurens KR, Cullen AE, Hodgins S. Meta-analyses of cognitive and motor function in youth aged 16 years and younger who subsequently develop schizophrenia. *Psychol Med.* 2012;42(4):743–755.
43. Peng Y, Zhang S, Zhou Y, *et al.* Abnormal functional connectivity based on nodes of the default mode network in first-episode drug-naive early-onset schizophrenia. *Psychiatry Res.* 2021;295:113578.
44. Hilland E, Johannessen C, Jonassen R, *et al.* Aberrant default mode connectivity in adolescents with early-onset psychosis: a resting state fMRI study. *Neuroimage Clin.* 2022;33:102881.
45. Selemon LD, Wang L, Nebel MB, Csernansky JG, Goldman-Rakic PS, Rakic P. Direct and indirect effects of fetal irradiation on cortical gray and white matter volume in the macaque. *Biol Psychiatry.* 2005;57(1):83–90.
46. Dong D, Yao D, Wang Y, *et al.* Compressed sensorimotor-to-transmodal hierarchical organization in schizophrenia. *Psychol Med.* 2021;1:14.
47. Dong HM, Margulies DS, Zuo XN, Holmes AJ. Shifting gradients of macroscale cortical organization mark the transition from childhood to adolescence. *Proc Natl Acad Sci USA.* 2021;118(28):e2024448118.
48. Rapoport JL, Giedd JN, Gogtay N. Neurodevelopmental model of schizophrenia: update 2012. *Mol Psychiatry.* 2012;17(12):1228–1238.
49. Driver DI, Thomas S, Gogtay N, Rapoport JL. Childhood-onset schizophrenia and early-onset schizophrenia spectrum disorders: an update. *Child Adolesc Psychiatr Clin N Am.* 2020;29(1):71–90.
50. Nicolson R, Rapoport JL. Childhood-onset schizophrenia: rare but worth studying. *Biol Psychiatry.* 1999;46(10):1418–1428.
51. Jones EG. Thalamic circuitry and thalamocortical synchrony. *Philos Trans R Soc Lond B Biol Sci.* 2002;357(1428):1659–1673.
52. Halassa MM, Sherman SM. Thalamocortical circuit motifs: a general framework. *Neuron.* 2019;103(5):762–770.
53. Garcia-Cabezas MA, Zikopoulos B, Barbas H. The Structural Model: a theory linking connections, plasticity, pathology, development and evolution of the cerebral cortex. *Brain Struct Funct.* 2019;224(3):985–1008.
54. Andreasen NC, O’Leary DS, Cizadlo T, *et al.* Schizophrenia and cognitive dysmetria: a positron-emission tomography study of dysfunctional prefrontal-thalamic-cerebellar circuitry. *Proc Natl Acad Sci USA.* 1996;93(18):9985–9990.
55. Andreasen NC, Paradiso S, O’Leary DS. “Cognitive dysmetria” as an integrative theory of schizophrenia: a dysfunction in cortical-subcortical-cerebellar circuitry? *Schizophr Bull.* 1998;24(2):203–218.
56. Andreasen NC. A unitary model of schizophrenia: Bleuler’s “fragmented phrene” as schizencephaly. *Arch Gen Psychiatry.* 1999;56(9):781–787.